Chapter 7

Summary and Future work

7.1 Summary

In this thesis I have utilized large-scale millimeter and mid- to far-infrared surveys to address a number of outstanding questions regarding the formation of low mass stars in molecular clouds, including:

(1) What are the global physical processes controlling the formation and support of prestellar cores, and their subsequent collapse into protostars?

(2) What are the initial conditions of prestellar cores in molecular clouds, and how do their properties change after protostellar formation?

(3) How do newly formed protostars evolve through the earliest phases; in particular, what are their mass accretion rates and timescales for evolution?

(4) How do the properties of dense cores depend on environmental factors such as the strength of turbulence?

Using Bolocam, a recently implemented bolometer array at the Caltech Submillimeter Observatory, I have surveyed the Perseus, Serpens, and Ophiuchus molecular clouds at $\lambda = 1.1$ mm, and developed methods to calibrate and analyze the resulting observations. These surveys have a resolution of $31''$ and cover the largest areas observed at millimeter or submillimeter wavelengths to date in each cloud: 7.5 deg^2 in Perseus, or 140 pc^2 at the adopted cloud distance of $d = 250$ pc, 10.8 deg^2 (50 pc^2 at $d = 125$ pc) in Ophiuchus, and 1.5 deg^2 (30 pc^2 at $d = 125$ pc) in Serpens. They are sensitive to dense sub-structures with mean particle density $\langle n \rangle \gtrsim 2 - 3 \times 10^4$ cm^{-3}

and contrast with the average background density of at least a factor of $30 - 100$. A total of 122 such 1.1 mm cores are detected in Perseus above a point source mass detection limit of 0.18 $M_\odot$, 44 cores in Ophiuchus above a detection limit of 0.1 $M_\odot$, and 35 cores in Serpens above a detection limit of 0.13 $M_\odot$. The total mass contained in dense cores is 285 $M_\odot$ in Perseus, 42 $M_\odot$ in Ophiuchus, and 92 $M_\odot$ in Serpens.

The Bolocam surveys were designed to cover the same regions as mid- and far-infrared *Spitzer* IRAC and MIPS maps of Perseus, Serpens, and Ophiuchus completed as part of the "Cores to Disks" Legacy project. Combining the *Spitzer* and Bolocam surveys provides wavelength coverage from $\lambda = 1.25 - 1100 \mu$m, and enables the separation of prestellar and protostellar cores, as well as the construction of well-sampled spectral energy distributions (SEDs) for cold protostellar candidates. This unprecedented, complete census of the youngest star forming objects in three diverse molecular clouds includes 108 prestellar cores, 43 Class 0 sources and 94 Class I sources. It is complete for all Class 0 objects that have envelope masses $M_{env} \gtrsim 0.2$ $M_\odot$, and for all Class I objects that have $M_{env} \gtrsim 0.1$ $M_\odot$. This unique sample enables the following investigations of questions (1) through (4) outlined above:

1. Two simple observational tests can distinguish between magnetic fields and turbulence as the dominant physical processes controlling the formation, support, and collapse of dense cores in molecular clouds: the prestellar core lifetime, and the existence of an A_V threshold. Surprisingly, the results of these tests seem to suggest conflicting interpretations. In all three clouds the lifetime of dense prestellar cores is approximately equal to the entire time spent in the embedded protostellar phase, $2 - 4 \times 10^5$ yr, or only a few free-fall timescales. Such a short prestellar core lifetime is inconsistent with the classic scenario of magnetic field support in which core evolution occurs on the ambipolar diffusion timescale of $t_{AD} \sim 10^7$ yr (Nakano, 1998). Thus the measured prestellar core lifetime argues for a dynamic, turbulent core formation process in these clouds.

On the other hand, the fact that dense cores are found only at high cloud column densities ($A_V \gtrsim 7$ mag) in all three clouds, and the observation of a true A_V threshold

in Ophiuchus at $A_V \sim 17$ mag, suggests that magnetic fields must also play some role in the formation of prestellar cores. As discussed in chapter 1, column density thresholds for star formation arise naturally if core collapse is moderated by ambipolar diffusion (Shu et al., 1987; McKee, 1989), but are difficult to reconcile with a turbulent paradigm (Johnstone et al., 2004).

Scenarios in which both magnetic fields and turbulence are important have been explored with numerical simulations; Vázquez-Semadeni et al. (2005) suggest that strong magnetic fields in turbulent clouds decrease the star formation efficiency without increasing the prestellar core lifetime. The fraction of total cloud mass contained in dense cores, an upper limit to the instantaneous star formation efficiency, is less than 10% in all three clouds, lower than typically predicted in turbulent simulations without magnetic fields (e.g., Klessen et al., 2000). Taken together, my results argue for turbulence being the dominant physical process in molecular clouds, but in the presence of magnetic fields that are strong enough (i.e. marginally sub-critical) to prevent core formation in low column density regions, and to lower the star formation efficiency to $< 10\%$.

2. The prestellar core mass distribution (CMD) is an important diagnostic of initial conditions, in that it may reveal whether feedback, dynamical, or core fragmentation processes are responsible for the form of the stellar initial mass function (IMF). I constructed the prestellar CMD by utilizing the combined starless core samples from all three clouds. The best fitting power law to the prestellar CMD for $M > 0.8\,\mathrm{M_\odot}$ has a slope of $\alpha = -2.5 \pm 0.2$, remarkably similar to recent measurements of the slope of the IMF for $M \gtrsim 0.5\,\mathrm{M_\odot}$: $\alpha = -2.4 - 2.8$ (Reid et al., 2002; Scalo, 1986). While such a similarity cannot rule out the importance of feedback or competitive accretion in determining the final masses of stars, it provides support for the hypothesis that stellar masses are directly linked to the masses of their parent cores. Furthermore, given my conclusion above that turbulence dominates core formation, this result indicates that the shape of the IMF is determined during the turbulent fragmentation of cloud material into dense cores. The ratio of the characteristic masses of the CMD and

IMF places a lower limit on the efficiency of core collapse of 25%.

Measured angular deconvolved sizes of starless cores indicate that the majority have radial density profiles that are substantially flatter than $\rho \propto r^{-2}$, predicted by Shu et al. (1987) for cores on the verge of collapse. My results support recent research showing that most starless cores are consistent with density power law indices of $p \lesssim 1.6$, or with flattened inner profiles such as Bonnor-Ebert spheres (e.g., Di Francesco et al., 2007).

A comparison of the starless and protostellar core populations in each cloud indicates that dense starless cores are already spatially clustered, and occur in regions of high cloud column density. Therefore, the initial spatial distribution of cores is not significantly altered by protostellar formation. In contrast, the mass distribution widens considerably after the formation of a central protostar, as determined from a comparison of the prestellar CMD to the protostellar CMD. Starless cores in Perseus have larger sizes and lower densities on average than protostellar cores for a similar range of masses, providing a simple explanation of how protostellar cores might have evolved from the starless cores in that cloud, by becoming smaller and denser at a constant mass. In Serpens, however, it is not clear how the relatively massive protostellar cores could have evolved from the current population of compact, low mass starless cores, suggesting that the future generation of stars in that cloud will have lower mass than those of the currently forming protostars. By contrast, cores in Ophiuchus appear to evolve very little after the formation of a central protostar.

3. To study the early evolution of protostars, observed source properties are compared to protostellar evolutionary models using the bolometric temperature-luminosity (T_{bol}–L_{bol}) diagram, the protostellar equivalent of the H-R diagram (Myers et al., 1998). Neither models with a constant mass accretion rate (Young & Evans, 2005), nor those with an exponentially declining rate (Myers et al., 1998) fit the observed population of Class I sources. In particular, Class I sources display a large spread in L_{bol} of 2–3 orders of magnitude, and there is a substantial population of low-luminosity Class I objects that cannot be explained by the general model prediction that L_{bol} should

peak during the Class I phase. This result provides strong evidence for episodic accretion during the Class I phase. Based on the number of sources with $L_{bol} < 0.1 \mathrm{L}_\odot$, protostars must spend approximately 25% of their Class I lifetime in a quiescent state.

Corresponding low-luminosity Class 0 sources are not observed; most Class 0 sources can be explained by a constant accretion rate model and masses from 0.3 to 3.0 $\mathrm{M}_\odot$. I find approximately half as many Class 0 as Class I sources in Perseus and Serpens, implying a Class 0 timescale of $1 - 2 \times 10^5$ yr. Thus there can be no very rapid early accretion truncating the Class 0 phase, as has been suggested by André & Montmerle (1994) and more recently by Froebrich et al. (2006). In fact, it appears unlikely that the *average* accretion rate drops by more than a factor of two from Class 0 to Class I. In Ophiuchus the fraction of Class 0 sources is much smaller: $N_{Class0}/N_{ClassI} \sim 0.1$. This difference may be due in part to overestimates of T_{bol} values derived without 160μm flux measurements, but more likely either the Class 0 phase is considerably shorter, or the star formation history is much more temporally variable, in Ophiuchus than in the other clouds.

4. With a few important exceptions, large environmental differences are not observed for the dense core populations. The majority of 1.1 mm cores are consistent with power law density profiles, at least on scales larger than the $31''$ Bolocam beam, and inferred power law indices are similar in each cloud ($p \sim 1.4 - 1.7$). Spatial clustering properties are also similar for all three clouds, with some evidence that clustering remains strong out to larger scales in Perseus. There is a larger range of measured core sizes and densities in Perseus, reflecting a wider variety of physical conditions and more distributed star formation in that cloud. The relationship between dense cores and the local cloud column density does vary from cloud to cloud, as 1.1 mm cores are found at considerably higher column densities in Ophiuchus than in Perseus or Serpens. More than 75% of cores are found at visual extinctions of $A_V \gtrsim 8$ mag in Perseus, $A_V \gtrsim 15$ mag in Serpens, and $A_V \gtrsim 20 - 23$ mag in Ophiuchus.

The measured core mass distributions (CMDs) display notable variations with environment. Cloud CMDs are well characterized by power law fits ($dN/dM \propto M^\alpha$)

above their empirically derived 50% completeness limits, resulting in slopes of $\alpha = -2.1 \pm 0.1$ in Perseus, $\alpha = -2.1 \pm 0.3$ in Ophiuchus, and $\alpha = -1.6 \pm 0.2$ in Serpens. The slope predicted for turbulent fragmentation, $\alpha \sim -2.4$ (e.g., Padoan & Nordlund, 2002), is similar to the measured slope for Perseus and Ophiuchus, but not for Serpens. Based on a two-sided Kolmogorov-Smirnov test, the core samples in Ophiuchus and Serpens are found to have a low probability (5%) being drawn from the same parent distribution of masses. Ballesteros-Paredes et al. (2006) argue that the shape of the CMD should depend on the turbulent properties of the cloud, with higher Mach numbers leading to a larger fraction of low mass cores. The relative shapes of the observed cloud CMDs, with the largest fraction of high mass cores in Serpens, the most turbulent cloud, are contrary to what would be expected from the simulations of Ballesteros-Paredes et al. (2006). While it seems likely turbulence is responsible for the formation of dense cores, and can explain the CMD in a general sense, the detailed dependence on Mach number is not well characterized by simulations.

The studies described in this thesis help to shed light on a number of problems in low mass star formation, while in turn raising new issues and highlighting the need for more precise, testable predictions from theory and simulations. Perhaps most surprising is the variation of core properties and protostellar evolution with environment for the three molecular clouds. In recent years much effort has gone into reproducing the short Class 0 lifetime originally measured in Ophiuchus, but the unprecedented sample assembled here suggests that Ophiuchus may be a special case, and the Class 0 lifetime is likely to be much longer in the majority of star-forming environments. While my results support the growing body of evidence that turbulence plays a very important role in the star formation process (e.g., Mac Low & Klessen, 2004), the distinction between magnetic fields and turbulence as the dominant physical forces in molecular clouds is not clear cut; apparently, the influence of magnetic fields must be accounted for in any complete model of turbulent star formation.

7.2   The Future

Closer collaboration between theorists, simulators, and observers is essential to fully understand the implications of the wealth of *Spitzer* data and large scale (sub)mm continuum and molecular line surveys made available in the last few years. In chapter 5, I compared core mass distributions from three molecular clouds to the results of turbulent fragmentation simulations, in order to test environmental dependencies and the agreement between simulations and observations. A straightforward method for compare other properties of the dense core populations to results from turbulent fragmentation simulations would be extremely useful. For example, the spatial distribution of cores could be compared using the two-point correlation function (e.g., §5.5.4), and the relationship between dense cores and the surrounding cloud density (e.g., §5.5.5). Having the ability to "observe" the output of simulations or models in the same way as real observations will provide a substantial step forward in our ability to constrain star formation models.

Another important area for improvement is the measurement of the starless core mass distribution to much lower masses, which is essential to further test the relationship between the IMF and the CMD. The CMD for dense 1.1 mm cores studied here begins to suffer from incompleteness at $M \sim 0.8$ $M_{\odot}$; to directly compare to the IMF characteristic mass of 0.25 $M_{\odot}$(Chabrier, 2005), more sensitive observations are needed. While the CMD of Alves et al. (2007) is complete to approximately 0.4 $M_{\odot}$, the dust extinction method used traces structures with relatively low density, and their sample may be contaminated by unbound cores and other diffuse structures. The upcoming SCUBA2 bolometer array and the ALMA interferometer will revolutionize this field, making it possible to detect prestellar cores with $M \ll 0.1$ $M_{\odot}$ over large scales and at high resolution. The coordination of these continuum data with molecular line observations to determine if observed cores are bound will enable a more detailed comparison between the CMD and the IMF.

In the remaining sections I outline in more detail a few projects inspired by the work in this thesis, which I intend to pursue in the next several years. Anticipated

lines of inquiry include the refinement of arguments made in this thesis, such as the lifetime of the Class 0 phase, and using the large sample compiled here to isolate unbiased subsets for more detailed study.

7.2.1 Main Accretion Phase Lifetime

The combination of c2d *Spitzer* maps and Bolocam 1 mm surveys made possible a calculation of the number of Class 0 sources in the Perseus, Serpens, and Ophiuchus molecular clouds, but in fact this analysis only begins to tie down the main accretion phase lifetime. A major source of uncertainty in this calculation is the treatment of close multiple sources, which are confused in the $31''$ resolution Bolocam data. Thus follow-up observations are necessary, particularly at high resolution.

Observations of a sample of 19 multiple protostars not previously observed at high resolution are currently underway with the Combined Array for Millimeter-wave Astronomy (CARMA) interferometer. Targets are identified from Bolocam *Spitzer* c2d maps of Perseus, Serpens, and Ophiuchus as two or more 24μm or 70μm sources within the radius of a single Bolocam 1 mm core (e.g., figure 6.2, Pers-Bolo 49). These high-resolution 3 mm continuum observations will determine the fraction of millimeter flux associated with each source, thus clarifying their evolutionary state. A more accurate accounting of the relative number of Class 0 and Class I sources will enable a refinement of the Class 0 lifetime estimate. Simultaneous observations of outflow-tracing molecular lines will give further insight into the evolutionary state of each source.

7.2.2 Tracing Structure Near the Protostar

The data presented in this thesis are sensitive to deeply embedded protostars and their surrounding envelopes, but they cannot probe the envelope on scales smaller than the $31''$ Bolocam beam. Very little is known about the small scale structure in most Class 0 sources, including whether they might be small-separation binaries. Directly resolving the structure around protostars on scales <100 AU is difficult, but

the amount of flux escaping at $\lambda \lesssim 50\mu$m from deeply embedded sources strongly constrains their innermost structure. Recently, evidence for a hole in the inner envelope of IRAS 16293-2422 was found by comparing the observed IRS spectrum with detailed radiative transfer models (figure 7.1, left; Jørgensen et al. 2005). Those data revealed an inner cavity that is slightly larger than the separation of this Class 0 binary.
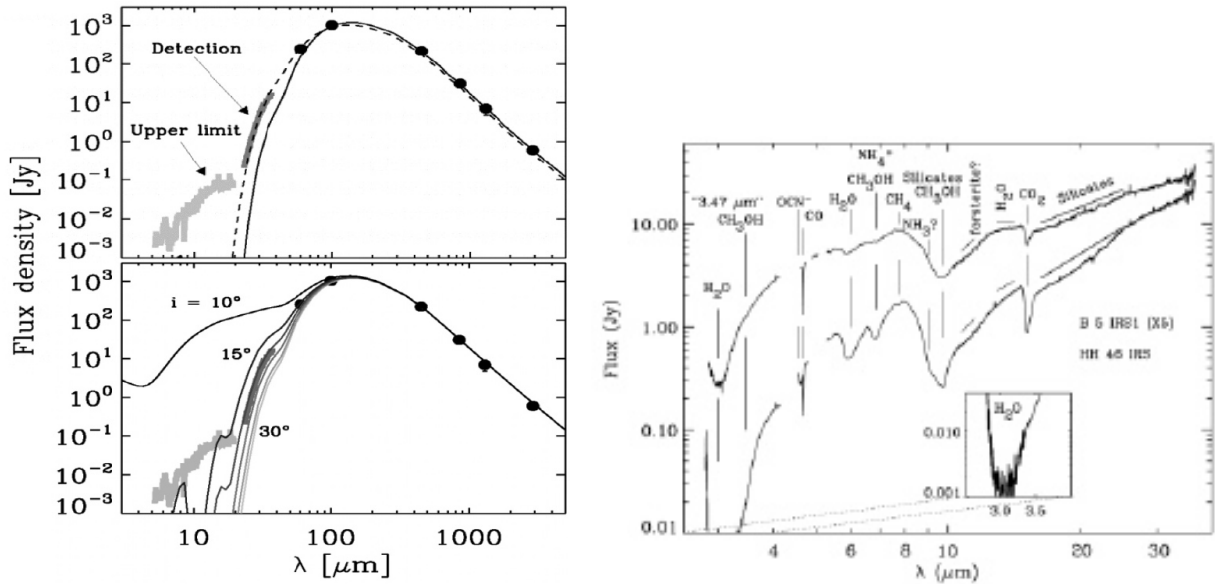

Figure 7.1 An example of using *Spitzer* IRS data to understand small scale structure in a Class 0 protostar. *Left top:* The SED of IRAS 16293-2422 from Jørgensen et al. (2005), compared to radiative transfer models with (dotted line) and without (solid line) a 600 AU inner cavity. The two models are only differentiated by the IRS spectrum (in dark gray). *Left bottom:* Similar, but showing the effects of an outflow cavity with varying inclination angle (all with opening angle 30°). *Right: Spitzer* IRS spectra of two embedded protostars from Boogert (2004), showing the silicate absorption at 10μm and other ice features.

The IRS spectrograph on *Spitzer* will be used to observe a sample of 25 Class 0 objects from Perseus, Serpens, and Ophiuchus, with the goal of determining the innermost envelope structure of deeply embedded protostars. IRS spectra will also reveal inner cavities in both binary and single sources, e.g., if the inner region has been cleared out, or flattened into a thin disk by rotation in the core. The sources to be observed are chosen from the Class 0 samples compiled in this thesis, and

include objects from a range of environments. A diverse sample like this one is very important, as only a few famous sources have been studied to date. To infer the innermost envelope structure, the spectral energy distribution (SED) from 3.6 to 1100μm must be combined with radiative transfer modeling (Shirley et al., 2002). Model inputs include the envelope inner radius, T_{eff} of the central source, and the density distribution of the envelope. The first two are constrained by the SED, but the latter requires resolved (sub)mm observations. High-resolution millimeter maps of these targets will be obtained with CARMA to tightly constrain the envelope density profile.

IRS observations will also reveal the spectral details of Class 0 SEDs from 7 to 37μm. Many of the Class 0 protostars identified here display a dip in the SED around 10μm, which is likely a silicate absorption feature in the envelope (figure 7.1, right; Boogert 2004), but could also be related to a conical outflow cavity (figure 7.1, left). It is tempting to assign those sources with minima at 10μm to a distinct phase within the Class 0 classification, but differences may simply be a function of cloud environment or outflow inclination angle. Correlations between observed source properties and evolutionary tracers such as T_{bol} will determine if the presence of a cavity, average cavity size, or spectral features from $7-37\mu$m change systematically with protostellar age.

7.2.3 Timescale for Disk Formation and the Disk Mass Fraction

Although disk-like structures have now been observed embedded within the envelopes of a few Class 0 sources, it is still not clear how soon after protostellar formation the disk appears. Separating the disk flux from that of the envelope is becoming more feasible with the improved uv coverage and sub-arcsecond resolution of current (sub)mm interferometers, which can resolve emission on small to large scales. Figure 7.2 shows an example of disentangling the disk and envelope contributions in a Class I protostar using the PdB Interferometer (from Harvey et al., 2003).
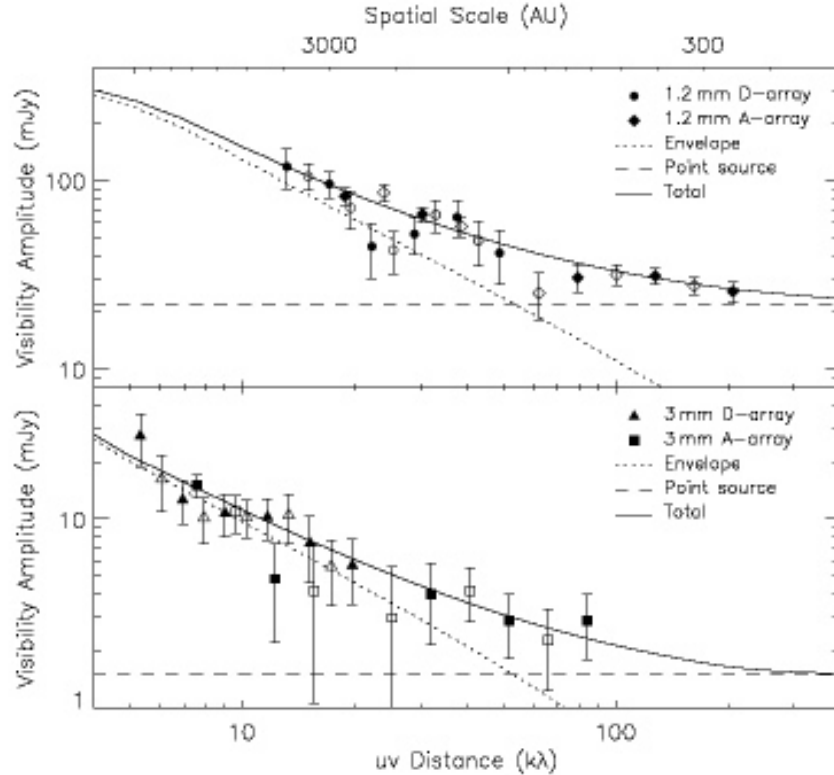
Figure 7.2 An example of separating disk and envelope contributions. IRAM PdBI interferometric observations at 1.2 and 3.0 mm are compared to a simple model consisting of a point-like disk (dashed line) and extended envelope (dotted line) (Harvey et al., 2003). CARMA observations will be sensitive to uv distances from 8.5 to 770 kλ at 1.3 mm, sampling the region most sensitive to the disk.

CARMA will be used to search for disks in a sample of 30 Class 0 sources in Perseus, Serpens, and Ophiuchus. This represents a larger and more unbiased sample than previous studies, and includes main accretion phase protostars at a range of ages. Class 0 disks are thought to have sizes of order $100 - 300$ AU (Chandler et al., 1995). Thus a resolution of at least 100 AU and uv coverage from ~ 10 to $\gtrsim 500$ kλ are required to adequately sample disk and envelope structures, both of which are achievable with CARMA. Millimeter continuum observations detect emission from dust grains in the disk and envelope; assuming that this emission is optically thin at $\lambda = 1 - 3$ mm, it provides a direct measure of mass. Mosaiced observations at $1-3$ mm will attempt to determine the total mass in the envelope and disk components in Class 0 objects.. Although dust emission is stronger at shorter wavelengths, the

possibility of grain grown in the disk makes observations at longer wavelengths (7 mm–2 cm, e.g., with the VLA) desirable as well.

Bibliography

Alves, J., Lombardi, M., & Lada, C. J. 2007, A&A, 462L, 17

André, P. & Montmerle, T. 1994, ApJ, 420, 837

Ballesteros-Paredes, J., Gazol, A., Kim, J., Klessen, R. S., Jappsen, A-K., & Tejero, E., 2006, ApJ, 637, 384

Boogert, A. C. A. 2004, ApJ, 154, 359

Chabrier, G. 2005 in The Stellar Initial Mass Function Fifty Years Later, editors E. Corbelli, F. Palla, and H. Zinnecker, p. 41

Chandler, C. J., Koerner, D. W., Sargent, A. I., Wood, D. O. S. 1995, ApJ, 449, 139

Di Francesco, J., Evans, N. J., II, Caselli, P., Myers, P. C., Shirley, Y., Aikawa, Y., & Tafalla, M. 2007, in Protostars and Planets V, editors B. Reipurth, D. Jewitt, and K. Keil, p. 17

Froebrich, D., Schmeja, S., Smith, M. D., & Klessen, R. S. 2006, MNRAS, 368, 435

Harvey, D. W. A., Wilner, D. J., Myers, P. C., Tafalla, M. 2003, ApJ, 596, 383

Johnstone, D., DiFrancesco, J., & Kirk, H. 2004, ApJ, 45, 611L

Jørgensen, J. K., Bourke, T. L., Myers, P. C., Schöier, F. L., van Dishoeck, E. F., Wilner, D. J. 2005, ApJ, 631, L77

Klessen, R. S., Heitsch, F., & Mac Low, M.-M. 2000, ApJ, 535, 887

Mac Low, M.-M., & Klessen, R. S. 2004, RevPhys, 76, 125

McKee, C. F. 1989, ApJ, 345, 782

Myers, P. C., Adams, F. C., Chen, H., Schaff, E. 1998, ApJ, 492, 703

Nakano, T. 1998, ApJ, 494, 587

Padoan, P., & Nordlund, Å. 2002, ApJ, 576, 870

Reid, I. N., Gizis, J. E., & Hawley, S. L. 2002, AJ, 124, 2721

Scalo, J. M. 1986, Fundam. Cosmic Phys., 11, 1

Shirley, Y. L., Evans, N. J., II, & Rawlings, J. M. C. 2002, ApJ, 575, 337

Shu, F. H., Adams, F. C., & Lizano, S. 1987, ARA&A, 25, 23

Vázquez-Semadeni, E., Kim, J., Shadmehri, M., & Ballesteros-Paredes, J. 2005, ApJ, 618, 344

Young, C. H. & Evans, N. J., II 2005